A comparison between 1 D electromagnetic modeling programs: a case history for Cristalino Iron-Oxide Copper Gold Deposit, Carajás Mineral Province, Brazil

Aline T. M. C. Silva (Universidade Federal de Minas Gerais), Mônica G. Von Huelsen (Universidade de Brasília), Umberto J. Travaglia Filho (Universidade de Brasília), Reinhardt A. Fuck (Universidade de Brasília)

Abstract

Cristalino (482 Mt @ 0.65% Cu and 0.06 g/t Au) is a world class Cu-Au IOCG deposit located in the Carajás Mineral Province. As extensive overburden cover makes exposure of the bedrock limited in Carajás region, geophysics plays a fundamental role in exploration. The detailed understand of the geophysical signature of the known deposits is the key for future exploration as the targets are getting deeper. For this work two methods were applied to the 1D electromagnetic inversion (programs ImagEM and EM1DTM) and 2.5D plate modeling (program Maxwell). The inversion results for Cristalino show that even if the deposit is not massive sulfide, it was effectively modeled and the method respond very well to the ore body. The electromagnetic signature of the deposit obtained by the plate modeling is of 21S for the high grade ore and 15S for the low grade ore, and a new target was identified at south of the main deposit. The anomalous body obtained by EM1DTM has the resistivity of 660 Ohm.m. Even though ImagEM is not quantitative accurate, it can map the resistivity contrast with a very good precision.

Introduction

The class of iron oxide-Cu-Au (IOCG) deposits has captured the attention of many mineral explorers in the last decades since the discovery of the giant Olympic Dam breccia-hosted iron oxide Cu-Au-UREE deposit in South Australia. There have been notable successes, and extensive exploration programs continue on most continents (Smith, 2002). They are often localized along fault splays off major, crustal scale extensional faults, but are located in diverse rock types, resulting in a wide variety of deposit styles and mineralogies (Hitzman, 2000).

The essential criteria are that IOCG deposits are formed by magmatic-hydrothermal processes, have Cu ± Au as economic metals, and are structurally controlled - commonly with breccias (Groves et al., 2010). The primary mineralogical characteristic of all deposits in this class is the abundance of magmatically sourced iron oxide, either magnetite or hematite. The presence of copper, as chalcopyrite is a primary economic characteristic. Due to the large influence of structural control, deposits of this type occur in many shapes, sizes and attitudes (Hitzman, 2000).

The Cristalino Cu-Au Deposit is located in the Carajás Neoarchean Domain, also known as Itacaiunas Belt, southeastern Amazonian Craton (Docegeo, 1988; Huhn et al., 1988) (Figure 1a).

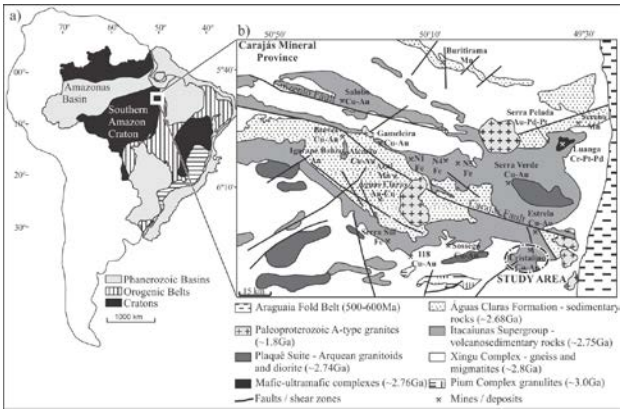

Figure 1. (a) Tectonic location of the Carajás Mineral Province at the southeastern margin of the Southern Amazon Craton, Brasil (Almeida et al., 1981), (b) Geologic Map of the Carajás Mineral Province showing the study area (Docegeo, 1988; Grainger et al., 2008).

Cristalino Deposit is hosted by a splay of the Carajás fault located in the southeastern part of Carajás Neoarchean Domain (Figure 1b). Its Cu-Au mineralization is hosted by hydrothermally altered mafic to felsic volcanic rocks interlayered with iron formation of a volcano-sedimentary sequence and was classified as an IOCG (Fe-Cu-Au-U-REE) deposit type. Granite, diorite and quartz-diorite intrude the volcano-sedimentary sequence (Figure 2; Huhn et al., 1999).

The deposit is estimated at 482 Mt @ 0.65% Cu and 0.06 g/t Au (NCL Brasil, 2005). The mineralization occurs in stockwork, stringer, breccias, disseminated in the host rock and filling fractures that cut the sequence. The main ore minerals are chalcopyrite and gold (Huhn et al., 1999). The geological model built from drilling information, as logging and assay, divided the ore body in high grade and low grade bodies (Figure 3).

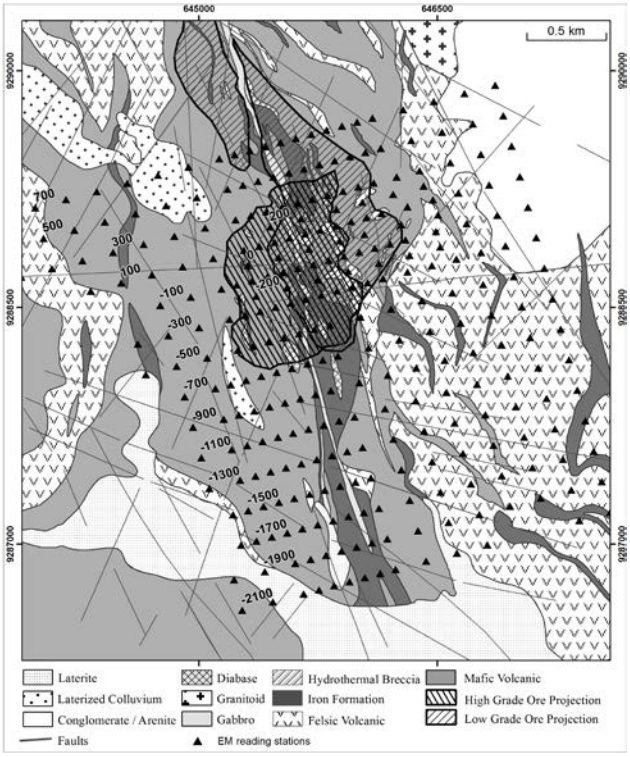

Figure 2. Lithological map of Cristalino Cu-Au Deposit showing the EM reading stations (Vale, 2004).

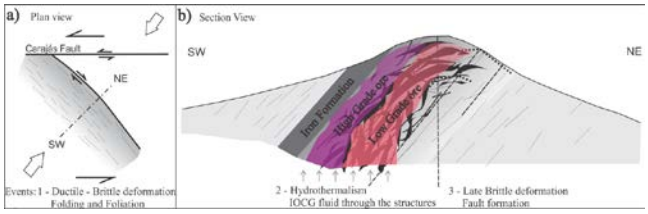

Figure 3. (a) Schematic plan view of Cristalino area showing the faults and direction of deformation, (b) Schematic geological section showing the hydrothermal mineralized zone and the events that formed the deposit (Adapted from Pinheiro, 2000).

Survey Data and Processing

The electromagnetic time-domain (TDEM) methods are very important for exploration of massive to semi-massive sulfide deposits. The area of Cristalino was covered by a ground TDEM survey aiming to identify the high conductivity zones (chalcopyrite + hydrothermal magnetite). The deposit area was covered by a detailed ground survey according to the specifications of table 1.

Table 1. Survey specifications over Cristalino Deposit.

System / Company	Config.	Line Spacing	Station Spacing	Year	Other specification
PROTEM/ Geomag	N75°E lines	100-200m	100-200m	1999	PROTEM 57, 30Hz

The ground EM data were acquired using the PROTEM 57 equipment, moving loop, centre in-loop readings X, Y and Z components, measuring dB/dt, current of 8 A, 20 time channels, loop side of 200 x 200 m, at the stations shown by figure 2.

The image of Z component channel 05 (Figure 4a) shows three anomalies of high amplitude, where the anomaly in the west of highest amplitude is due to the Laterized Colluvium. The central anomaly is the deposit and the anomaly to the south has the same signature of the deposit.

The anomaly corresponding to the conductive overburden decreases until it no longer appears after channel 10 of the Z component, and the anomalies corresponding to the mineralized zone have its area increased with increasing depth (Figures 4b to d), being strongly associated to the high grade ore which was modeled using the information of more than 300 drill holes.

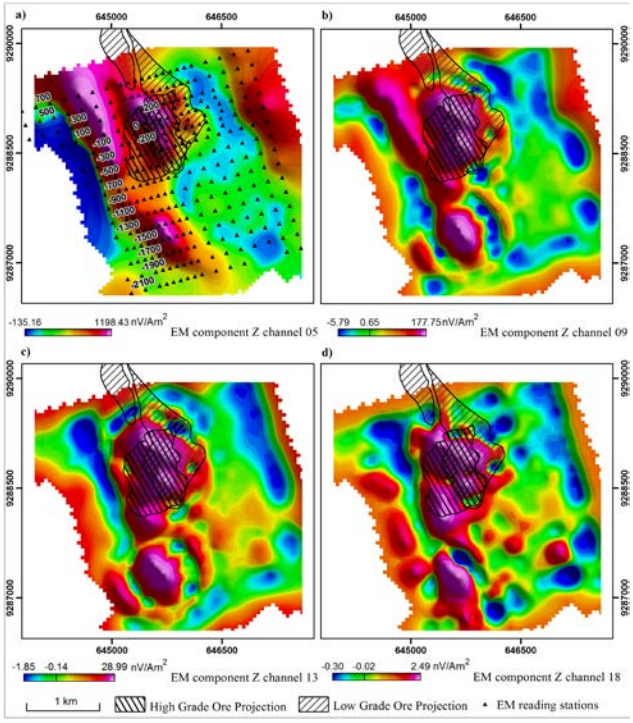

Figure 4. (a) Image of the ground electromagnetic component Z channel 05, (b) Image of the ground electromagnetic component Z channel 09, (c) Image of the ground electromagnetic component Z channel 13, and (d) Image of the ground electromagnetic component Z channel 18.

Modeling Programs

The electromagnetic data set at Cristalino was inverted by using approaches in inverse theory as described by Oldenburg and Li (2007). The earth is discretized into a large number of rectangular cells of constant physical properties and whose size is smaller than the resolution of the survey. The aim of the inversion algorithm is to

construct the simplest model that adequately reproduces the observations. To confront the nonuniquess, the inverse problem is formulated to minimize an objective function of the model subject to adequately fit the data.

The ground electromagnetic (EM) data have been forward modeled using the software Maxwell from EMIT (ElectroMagnetic Imaging Technology, 2011) and inverted using two different 1-D algorithms, the EM1DTM 1.0 from UBC (University of British Columbia) (Farquharson, 2006) and the ImagEM, under development by UnB (Universidade de Brasília) (Travaglia Filho, 2012).

The plate forward modeling was important to define plate size, azimuth and dip, which adequately fits the data. The EM1DTM program allows the use of a wide set of transmitter/receiver configuration, waveforms and time windows to give an electrical conductivity model. The Earth models are composed of layers of uniform conductivity with fixed interface depths. The value of the conductivity in each layer is sought by the inversion. Each sounding is inverted independently for a one-dimensional model under the sounding location, these can be viewed directly as a composite two-dimensional image for the whole line. The Huber M-measure is used for data misfit and Ekblom p-measure for model structure, which allow for a whole suite of variations, from the traditional sum-of-squares measures, to more robust measures which can ignore outliers in the observations and which can generate piecewise-constant models (Farquharson and Oldenburg, 1998). Four possible methods for determining the degree of regularization are possible: (1) the trade-off parameter is specified by the user, either as a single constant value, or with a cooling schedule to some final value, (2) the trade-off parameter is automatically chosen to achieve a user-supplied target misfit, (3) the trade-off parameter is automatically chosen using the GCV (generalized cross-validation) criterion, or (4) the trade-off parameter is automatically chosen using the L-curve criterion (Farquharson, 2006).

The ImagEM was initially based on the RAMPRES program (Sandberg, 1988; Von Huelsen, 2007), the program works for in-loop configuration when the receiver coil is concentric to the transmitter coil. It calculates the apparent resistivity applying the secant method and does not take any a priori information (Travaglia Filho, 2012).

The formulation is from Frischknecht and Raab (1984), it first calculates the resistivity for each measured time channel using different equations for early and late time, and then it takes the result to find the apparent resistivity through secant method with many numbers of iterations for each channel.

For the channels the user defines as early time, the program applies the equation:

$$\rho_{ET} = \frac{r_T^3 \; dB_z/dt}{3a_r}, \quad (1)$$

ρ_{ET} = resistivity of early time channels, r_T = transmitter radius, dB_z/dt = the electromagnetic field decay in Z direction measured in the equipment, and a_r = effective area of the receiver.

For the late time channels, when the secondary field is smaller, the program applies the equation for each channel:

$$\rho_{LT} = \frac{\mu_0}{4\pi t_n}\left(\frac{4\mu_0 \; Tm}{t \; dB_z/dt}\right), \quad (2)$$

ρ_{LT} = resistivity of late time channels, μ_0 = magnetic permeability of free space, Tm = transmitter dipole moment, and tn = time at channel n (n depends on the number of channels of the system).

The next step is to take the calculated ρ and apply in the equation:

$$\rho_{a_n} = \frac{\left(\frac{\mu_0 r_T a_r \, 0.886226}{\delta a_T}\right)(1-2R)\left[\left(\frac{\mu_0 r_T^2}{t_n x}\right)^{k+1.5} - \left(\frac{\mu_0 r_T^2}{t_n + \delta x}\right)^{k+1.5}\right]}{4^k k! \, (2k+5)\,(2k+3)}, \quad (3)$$

ρ_{a_n} = apparent resistivity of layer n (the number of layers is equal the number of channels), δ = ramp turn-off time, aT = transmitter coil area, k = number of the iteration, R = the difference of the division k/2, and x = log ρ (for the early time channels is log ρET and for late time channels log ρLT). This equation can reach up to 70 iterations using the secant method and is applied to every channel. At this point, the program has 20 values of apparent resistivity, the last part is to find the depth associated to each one.

There are many ways of calculating depth associated to a secondary electromagnetic field. The program ImagEM uses a formulation form Eaton (1989):

$$d_n = 150\sqrt{t_n \, \rho_{a_n}}, \quad (4)$$

dn = depth of layer n (the number of layers is equal the number of channels).

Each sounding is inverted independently for a one-dimensional model under the sounding location, with the sequence of one-dimensional models written out, these can be viewed directly as a composite two-dimensional image.

Results

A plate model was built for the ground TDEM data using channels 10 to 20 because of the strong overburden response of channels 1 to 9. The plate model aims to fit all three components and it is very accurate for dip, azimuth and extents.

The plate model delineates the general framework of the deposit and the modeled conductivities vary from 3 to 21 Siemens (Figure 5a). Considering that the mineralization style is not massive but instead a mixture of styles, the modeled plates are not interpreted as single layers of massive sulfide, but as the average of the sum of the response of all styles in the mineralized zone. Figure 5b shows that the best plate (line -300, 21 Siemens) maps the top of the high-grade ore having the same dip of this zone.

Plate of line 500 (18 Siemens) also seems to map the top of the low-grade ore with a slight change in the azimuth in relation to the previous plate, reflecting the change in azimuth of the low-grade ore that trends more to northwest.

The weaker plates are related to the iron formation bed (Figure 5c). As observed in the EM images of the previous section, there is an anomaly to the south of the deposit that is associated to a 15 Siemens plate (line -1500). It trends approximately east-west, a different azimuth of the deposit and the two drill holes in the region do not intercept significant mineralization. The holes there are almost parallel to the plate and could have missed the target (Figure 5d).

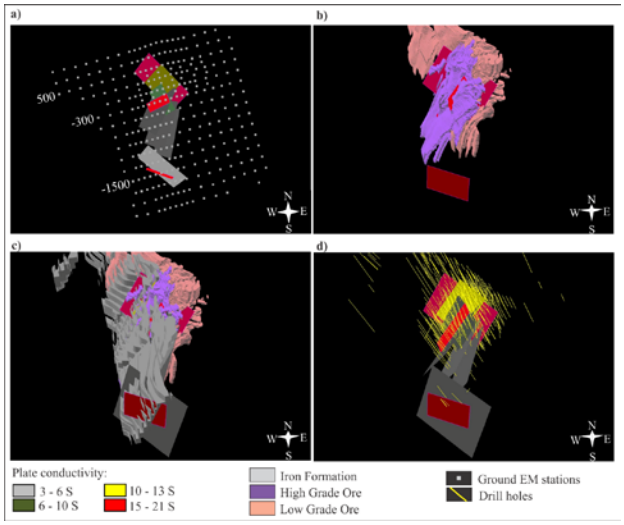

Figure 5. (a) Ground EM stations and the modeled plates, (b) the best conductivity plates with the high and low-grade ore, (c) the plates with the high and low-grade ore and the iron formation, and (d) the plates with all drill holes of the deposit.

The EM1DTM inversion behaved well for every station, where Phi d (misfit) decreased, Phi m (model norm) increased every iteration and observed data are of the same order of magnitude of the predicted data. For data misfit Huber norm was used because it is a robust misfit measurement that is less influenced by outliers. The inversion type used was the fixed-trade off cooling schedule, where it starts with a large tradeoff parameter and reduces it in every iteration. For the model norm the alpha-s was lowered and alpha-z raised to force the model to be smoother. The starting model that was used went to 4000 meters using 100 layers at 6000 Ohm-m. This model was used as both the starting model and the reference model for all soundings. Each sounding was inverted independently for a one-dimensional model under the sounding location; the resistivity values of the layers under the soundings were gridded into a two-dimensional section of 50x50m and into a three-dimensional mesh of 50x50x50 m cell size.

Figure 6a shows the low resistivity body obtained (660 Ohm.m), it has a very good fit with the high-grade ore extents and with high + low-grade ore thickness (Figure 6a, b).

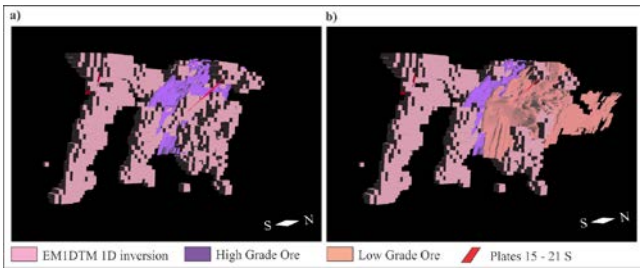

Figure 6. (a) Cut-off of 660 Ohm.m body with the high-grade ore, and (b) Cut-off of 660 Ohm.m body with the high-grade and low-grade ore.

As the ImagEM output is not quantitative but instead a qualitative result focused on showing the anomalous region, the resistivity values are going to be referred as low or high. Each sounding was inverted independently for a one-dimensional model under the sounding location. The recovered resistivity values of the layers under the soundings were gridded into a two-dimensional section of 50x50m and into a three-dimensional mesh of 50x50x50 m cell size.

Figure 8a shows the main low resistivity body of the inversion, the overburden was well and continuously modeled. The main part of the model is spatially coincident with the high-grade ore (Figure 8b) and does a good job on mapping its lateral extents but the dip is vertical, while the high-grade ore is west dipping. However, the Z component is the only one considered for the inversion.

The low resistivity body has the thickness very similar to the thickness of the orebody, high and low grade (Figure 4.10b) meaning that the model could pick the response of both. Although the body is continuous at shallower depths, it splits into two when it gets deeper. This deeper part of the deposit was not drilled yet but this information can be used as a guide to focus the drilling where the model indicates the ore is continuous. The anomaly to the south of the deposit (15S plate and 660 Ohm.m) shows up as a very consistent low resistivity body, as deep as the deposit but much narrower.

The result of the 1D inversion using EM1DTM is identical to the result of ImagEM. Although EM1DTM gives more detailed structures, it can be observed that the overburden response was not continuously modeled as in the ImagEM model.

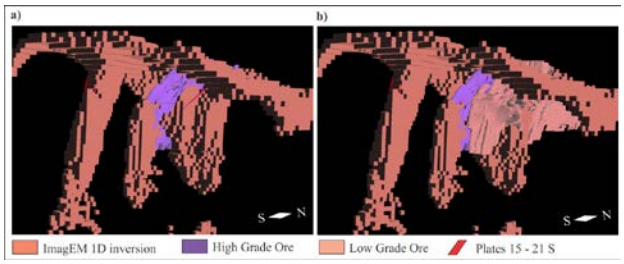

Figure 7. (a) Low resistivity body with the high-grade ore, and (b) Low resistivity body with the high-grade and low-grade ore.

Discussion

Accurately differentiating bedrock conductor from overburden conductors is one of the major strategies that have to be followed for metal exploration in the Amazon region. The inversion results for Cristalino show that even if the deposit is not massive sulfide, it was effectively modeled and the methods respond very well to the ore body, especially to the high-grade ore. All electromagnetic models could map its northern and southern extents with good accuracy. The electromagnetic signature of the deposit obtained by the plate modeling is 21S for the high grade ore and 15S for the low grade ore.

When comparing the EM modeling processes it can be seen that Maxwell is very sensitive to the user's experience. Thus, the model can be variable from user to user and depending on the complexity of the data, it takes one day to model each survey line. Even though the target in this case study is not massive mineralization, Maxwell does a very good job on mapping the ore zone. However, this work evidences that integration with other data shows that if the drill holes are planned just considering the plate model, the best part of the target can be missed, considering that the most conductive plate in Cristalino is at the top of the high-grade ore zone.

EM1DTM program also depends a lot on the users experience on inversion and on the software configuration to find the best parameters for the dataset that is being used. One advantage is that the program accepts all kinds of survey configuration but the input data format the program requires takes a long time from the user to get the data ready.

ImagEM uses a format similar to the one delivered by the contractors. It does not need any experience from the user and runs the modeling very fast. This is an advantage when fast results are needed to plan the continuity of the drilling program. The greatest contribution of this work shows that the program developed by the Electromagnetic Interpretation Research Group of Universidade de Brasilia can achieve results very similar to the results from EM1DTM nine times faster, even though its quantitative result are not accurate.

A new target, with the same signature of the deposit was found to the south of the main ore body. This target has few drill holes that have not intercepted mineralization, but the geophysical inversion results show it should be better investigated.

To improve mineral exploration success, there is an accepted need to increase the discovery space by exploring under cover and to greater depths, using 3D geological modelling supported by multiple geophysical data. The resistivity signature found for Cristalino can be used as guide or reference models to identify a number of localities in the subsurface with similar geophysical signature in the same geological environment as Cristalino deposit. These locations could be considered as potential targets and are candidates for further exploration.

Acknowledgements

We thank Vale S/A for granting the permission to use geophysical and geological data for academic purposes. The colleagues from Vale S/A for all support during the research, the colleagues from Universidade de Brasilia. Reinhardt A. Fuck acknowledges CNPq research fellowship. Corrections and suggestions by Adalene Silva, Renato Cordani helped improve this abstract.

References

Docegeo. 1988. Província Mineral de Carajás. Litoestratigrafia e principais depósitos minerais. 35º Congresso Brasileiro de Geologia, 11-54. Belém.

Eaton P. A. and Hohmann G. W. 1989. A rapid inversion technique for transient elec-tromagnetic soundings. Physics of the Earth Planetary Interiors, 53, 384-404.

ElectroMagnetic Imaging Technology (EMIT). Maxwell - Industry Standard Geophysical EM Data Modeling. http://www.electromag.com.au/maxwell.php, accessed 15 July 2011.

Farquharson C.G. and Oldenburg D.W. 1998. Nonlinear inversion using general measures of data misfit and model structure, Geophysical Journal International, 134, 213–227.

Farquharson C. G. 2006. Background for Program "EM1DTM" Version 1.0, developed under the consortium research project: Time Domain Inversion and Modeling of electromagnetic Data. Geophysical Inversion Facility, Department of Earth & Ocean Sciences, University of British Columbia (UBC - GIF), Vancouver, Canada.

Frischknecht F. C. and Raab P. V. 1984. Time domain electromagnetic soundings at the Nevada test site. Geophysics 49, 981-992.

Grainger C. J., Groves D. I., Tallarico F. H. and Fletcher I. R. 2008. Metallogenesis of the Carajás Mineral Province, Southern Amazon Craton, Brazil: Varying styles of Archean through Paleoproterozoic to Neoproterozoic base- and precious-metal mineralization. Ore Geology Reviews, 33, 451-489.

Groves D. I., Bierlein F. P., Meinert L. D. and Hitzman, M. W. 2010. Iron Oxide Copper-Gold (IOCG) Deposits through Earth History: Implications for Origin, Lithospheric

Setting, and Distinction from Other Epigenetic Iron Oxide Deposits. Economic Geology, 105, 641-654.

Hitzman M. W. 2000. Iron Oxide-Cu-Au Deposits: What, Where, When and Why. In: T. M. Porter (Ed.), Hydrothermal Iron Oxide Copper-Gold & Related Deposits: A Global Perspective (Vol. 1, pp. 9-25). Adelaide.

Huhn S. R., Santos A. B., Amaral A. F., Ledsham E. J., Gougêa J. L. and Martins L. P. 1988. O terreno "granito greenstone" da região de RioMaria - Sul do Pará. XXXV Congresso Brasileiro de Geologia, 3, pp. 1438-1452. Belém.

Huhn S. R., Souza C. I., Albuquerque M. C., Leal E. D., and Brustolin V. 1999. Descoberta do depósito Cu(Au) Cristalino: geologia e mineralização associada - Região da Serra do Rabo-Carajás- PA. VI Simpósio de Geologia da Amazônia, (pp. 140-143). Manaus.

NCL Brasil. 2005. Revision de La Estimación de Recursos del Proyecto Cristalino. Vale S.A Internal Report, 1-103.

Oldenburg D. W. and Y. Li. 2007. Inversion for Applied Geophysics: A Tutorial. http://www.eos.ubc.ca/ubcgif/iag/tutorials/tutorial-v9.pdf (accessed 10 January 2011).

Pinheiro R. V. L., 2000. Relatório de Consultoria Técnica. Projeto Cristalino - Serra dos Carajás / PA. Vale S.A Internal Report, 1-52.

Sandberg S. K., 1988. Microcomputer software for the processing and forward modeling of transient electromagnetic data taken in the central loop sounding configuration: New Jersey Geological Survey Open-File Report 88-1.

Smith R. 2002. Geophysics of Iron Oxide Copper-Gold Deposits. In: T. M. Porter (Ed.), Hydrothermal Iron Oxide Copper-Gold & Related Deposits: A Global Perspective (Vol. 2, pp. 357-367). Adelaide: PGC Publishing.

Travaglia Filho U. J. 2012. Desenvolvimento e implementação de software para obtenção da resistividade pela profundidade de dados TDEM. Master Dissertation nº 28, Instituto de Geociências - Universidade de Brasília - UnB, 1-102.

Vale S.A. 2004. Relatório de reavaliação de reservas estudo de pré-viabilidade - Projeto Cristalino. Vale S.A. Internal Report, 1-164.

Von Huelsen M. G. V. 2007. Interpretação de Dados de Eletromagnetometria Aeroeletrotransportada (AEM) do Sistema GEOTEM (Domínio do Tempo). Doctoral Thesis no 80, Instituto de Geociências - Universidade de Brasília - UnB, 1-202.